A Photonic Approach to Linearly Chirped Microwave Waveform Generation With an Extended Temporal Duration

Jiejun Zhang, *Student Member, IEEE*, Olympio Lucchini Coutinho, *Member, IEEE*, and Jianping Yao, *Fellow, IEEE*

***Abstract*— A photonic approach to linearly chirped microwave waveform generation with an extended temporal duration is proposed and experimentally demonstrated. The linearly chirped microwave waveform generation is realized based on spectral-shaping and wavelength-to-time mapping, in which a Fabry–Perot (FP) interferometer with a linearly increasing or decreasing free spectral range is used to as a spectral shaper, and the wavelength-to-time mapping is realized using a recirculating dispersive loop with a large equivalent dispersion coefficient realized by allowing the spectrally shaped optical pulse to travel in the dispersive loop multiple times. The generation of two linearly chirped microwave waveforms at two different frequency bands with two temporal durations of 25 and 42 ns and a time-bandwidth product (TBWP) of 210 is experimentally demonstrated.**

***Index Terms*— Chirped waveform generation, fiber Bragg grating, microwave photonics, time-bandwidth product (TBWP), wavelength-to-time mapping.**

I. Introduction

LARGE time-bandwidth product (TBWP) microwave waveforms can find numerous applications in radar [1], [2], spread-spectrum communications [3], microwave computed tomography [4], and modern instrumentation. For example, in a radar system, a linearly chirped microwave waveform that has a large TBWP can be used to improve the range resolution. Linearly chirped microwave waveforms are commonly generated by electronic means by which the temporal duration can be long. However, due to the limited speed of electronic circuits, the bandwidth and the central frequency of a linearly chirped microwave waveform generated electronically are usually limited to a few gigahertz [5]–[7]. A linearly chirped microwave waveform with a bandwidth and central frequency as high as tens or hundreds of GHz is needed to improve the spatial resolution in a modern radar system.

Recently, numerous photonic techniques have been proposed and demonstrated to the generation of large TBWP microwave waveforms [8], such as space-to-time pulse shaping [9]–[11], spectral-shaping and wavelength-to-time mapping [12]–[19], temporal pulse shaping [20], optical heterodyne [21], and using a microwave photonic filter [22] or an optoelectronic oscillator (OEO) [23]. A space-to-time pulse-shaping system is usually implemented with a spatial light modulator (SLM), which provides flexibility in updating in real time the pattern on the SLM and enables the generation of an arbitrary microwave waveform. The major limitations of using an SLM are the relatively high loss and large size [9], [10]. Although the SLM in a space-to-time pulse-shaping system can be replaced by an arrayed waveguide grating, the duration of the generated waveform is still limited, in a range of tens of picoseconds, due to the relatively small channel number of an arrayed waveguide grating, developed usually for wavelength-division multiplexing (WDM) communications applications [11]. Microwave waveform generation by temporal pulse shaping, using a microwave photonic filter, or an OEO, also has the limitation of small temporal duration. Microwave waveforms generated by optically heterodyning two optical waveforms from two laser sources have poor phase-noise performance [21] since the optical waveforms from two free-running laser sources are not phase correlated, or a sophisticated optical phase-locked loop (OPLL) should be used to lock the phase terms of the two laser sources, making the system complicated and costly.

On the other hand, a spectral-shaping and wavelength-to-time mapping waveform generation system is usually simpler, more flexible, and more cost effective as compared with the systems based on other techniques. In spectral-shaping and wavelength-to-time mapping, the spectral shaper, which is an optical filter designed with a specific spectral response, is used to change the spectrum of an ultra-short pulse. The spectrum of the spectrally shaped pulse can be mapped to the time domain by using a dispersive element, to generate a temporal waveform with a shape that is identical to the spectrum of the spectrally shaped pulse. Hence, to generate a linearly chirped microwave waveform, the optical filter should have a spectral response with a free spectral range that is linearly increasing or decreasing. In [12], a fiber-optic spectral shaper with a Michelson interferometer structure that

Manuscript received June 15, 2015; revised September 17, 2015, November 16, 2015, January 23, 2016, and February 25, 2016; accepted April 22, 2016. Date of publication May 6, 2016; date of current version June 2, 2016. This work was supported by the Natural Science and Engineering Research Council (NSERC) of Canada. The work of J. Zhang was supported by the China Scholarship Council.

J. Zhang and J. Yao are with the Microwave Photonics Research Laboratory, School of Electrical Engineering and Computer Science, University of Ottawa, Ottawa, ON, Canada K1N 6N5 (e-mail: jpyao@eecs.uottawa.ca).

O. L. Coutinho is with the Microwave Photonics Research Laboratory, School of Electrical Engineering and Computer Science, University of Ottawa, Ottawa, ON, Canada K1N 6N5, and also with the Instituto Tecnológico de Aeronáutica, São José dos Campos 12228-900, Brazil.

Color versions of one or more of the figures in this paper are available online at http://ieeexplore.ieee.org.

Digital Object Identifier 10.1109/TMTT.2016.2558648

uses two linearly chirped fiber Bragg gratings (LCFBGs) as two optical reflectors was demonstrated for linearly chirped microwave waveform generation. Due to the wavelength-dependent arm length difference of the Michelson interferometer, a linearly decreasing free spectral range is achieved, which is used for linearly chirped microwave waveform generation. In addition to the operation as two reflectors, the LCFBGs also function jointly as a dispersive element that can perform linear wavelength-to-time mapping. A TBWP of around 15 for the generated linearly chirped microwave waveform was achieved. In [13], two LCFBGs with different chirp rates that are fabricated and superimposed in a fiber to function as a spectral shaper. The two LCFBGs are used to constitute a Fabry–Perot (FP) cavity that has a linearly decreasing or increasing free spectral range due to the wavelength-dependent cavity length. A linearly chirped microwave waveform with a TBWP of 37.5 was achieved using the spectral shaper. In [14], a spectral shaper implemented using a Sagnac loop mirror with an LCFBG in the loop was reported. Again, the free spectral range of the spectral shaper is linearly decreasing or increasing due to the wavelength-dependent loop length. The TBWP of the experimentally generated linearly chirped microwave waveform was 44.8. In [15] , a tilted fiber Bragg grating (TFBG) fabricated in an erbium/ytterbium co-doped fiber was used as a spectral shaper, of which the spectral response can be tuned by optically pumping the TFBG. A linearly chirped microwave waveform with a tunable chirp rate from 1.8 to 7 GHz/ns was experimentally generated. In [16], a reconfigurable waveform generator with a bandwidth up to 60 GHz was realized using a silicon photonic chip. However, the waveforms generated in [15] and [16] are limited to have a temporal duration of 1 ns with a TBWP of less than 60. In [17], microwave waveform generation based on spectral-shaping and wavelength-to-time mapping was proposed, in which an electrically stabilized Mach–Zehnder interferometer (MZI) was used to spectrally shape the spectrum of a short optical pulse and a dispersion compensating fiber (DCF) was used to perform wavelength-to-time mapping. A linearly chirped microwave waveform with a temporal duration of 16 ns and a TBWP of 589 were achieved. Using a similar scheme, a TBWP of 600 was achieved thanks to the use of a photodiode with a large bandwidth of over 175 GHz [18]. However, the temporal duration of only 15 ns was still small for many applications. In [19], a linearly chirped microwave waveform with an arbitrarily long temporal duration was achieved by stitching a series of individual linearly chirped microwave waveforms with different initial phases. In the system in [19], an individual linearly chirped microwave waveform was generated based on spectral-shaping and wavelength-to-time mapping, in which a programmable optical filter and two modulators were employed. The system is very complicated. In addition, the temporal duration of an individual linearly chirped microwave waveform was only 5 ns, which was again limited by the small dispersion of the dispersive device for wavelength-to-time mapping. Although the techniques in [12]–[19] can be used to generate a wideband linearly chirped microwave waveform at a high carrier frequency of over tens of GHz, the temporal duration is small, which is fundamentally limited by the achievable maximum time delay of the dispersive device used for wavelength-to-time mapping. For example, the maximum time delay of an LCFBG is only a few nanoseconds, limited by its physical length [24]. Although a DCF with a length of tens of kilometers can achieve a larger dispersion, the high insertion loss needs to be compensated by a fiber amplifier, such as a distributed Raman amplifier, making the system very complicated [25]. For many applications, a simple and cost-effective approach to generate a microsecond or sub-millisecond long microwave waveform is needed.

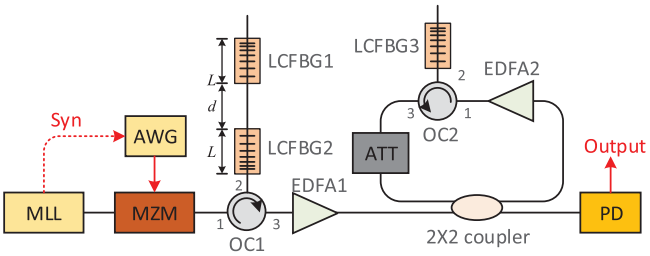

Fig. 1. Schematic diagram of the microwave waveform generation system. Synchronization: Syn; mode-locked laser: MLL; arbitrary waveform generator: AWG; Mach–Zehnder modulator: MZM; optical circulator: OC; linearly chirped fiber Bragg grating: LCFBG; attenuator: ATT; erbium-doped fiber amplifier: EDFA; photodetector: PD.

In this paper, a microwave waveform generator to generate a linearly chirped microwave waveform with an extended temporal duration by a repetitive multi-time use of an LCFBG in a fiber-optic recirculating loop is proposed and experimentally demonstrated. In our recent work reported in [26], a simple experiment was performed to prove the concept. In this paper, a comprehensive analysis is provided, which is then verified by more detailed experiments. In addition to the increase in the temporal duration, we also demonstrate that the central frequency of the generated linearly chirped microwave waveform can be tuned. In the proposed system, the spectral shaper is an FP interferometer incorporating two LCFBGs with complementary chirps to constitute an FP cavity with a linearly decreasing or increasing free spectral range. The spectrum of an ultra-short optical pulse is shaped by the FP interferometer. The pulse is then directed into a dispersive loop consisting of a third LCFBG. Since the optical pulse is temporally stretched multiple times when reflected by the third LCFBG multiple times, a linearly chirped microwave waveform with an extended temporal duration that exceeds the physical length of the third LCFBG can be generated. Note that although a similar dispersive loop has been used in [24], it is for a different application where fast signal sampling is implemented.

This paper is organized as follows. The operation principle of the proposed system is theoretically analyzed in Section II. An experiment to verify the operation of the proposed system is reported in Section III. A conclusion is drawn in Section IV.

II. Principle

Fig. 1 shows the schematic diagram of the microwave waveform generation system. An ultra-short optical pulse train is generated by a mode-locked laser (MLL) source. A repetition-rate-reduction module consisting of a Mach–Zehnder modulator (MZM) and an arbitrary waveform generator (AWG) is

used to realize the repetition rate reduction of the pulse train to avoid the overlapping of adjacent pulses when temporally stretched by the LCFBG in the dispersive loop. A gate signal is generated by an AWG with a repetition rate equal to that of the repetition-rate-reduced pulse train. The pulse train is then sent via an optical circulator (OC1) to an FP interferometer formed by two complementary LCFBGs (LCFBG1 and LCFBG2), which is used as the spectral shaper. An erbium-doped fiber amplifier (EDFA1) is employed after the MZM to compensate for the loss of the repetition-rate-reduction module. The pulse train is then launched into a dispersive loop, in which a third LCFBG (LCFBG3) is incorporated via a second optical circulator (OC2). In the dispersive loop, a second EDFA (EDFA2) is employed to provide an optical gain, followed by an attenuator (ATT) to balance the gain to be slightly less than 1 to avoid lasing. The temporally stretched pulse is finally detected by a photodetector via a 2×2 optical coupler. A linearly chirped microwave waveform with an extended temporal duration is obtained at the output of the photodetector.

Assuming that the dispersion coefficients of LCFBG1 and LCFBG2 are, respectively, $\ddot{\Phi}_1$ and $-\ddot{\Phi}_1$ when looking into from the second port of OC1, the cavity length of the FP interferometer for a light wave with an angular frequency of ω is given by [24]

$$L(\omega) = d + \frac{2c\tau(\omega)}{n_{\text{eff}}} = d + \frac{2c\ddot{\Phi}_1(\omega - \omega_s)}{n_{\text{eff}}} \tag{1}$$

where $\tau(\omega)$ is the time delay caused by LCFBG1 and LCFBG2 for a lightwave with an angular frequency of ω resonating in the FP interferometer; c is the light velocity in vacuum; n_{eff} is the effective refractive index of the optical fiber; and ω_s denote the lowest optical angular frequencies within the reflection bands of LCFBG1 and LCFBG2.

The free spectral range of the FP interferometer can then be calculated by

$$\omega_{\text{FSR}} = \frac{2\pi c}{2n_{\text{eff}} L(\omega)} = \frac{\pi c}{n_{\text{eff}} d + 2c\ddot{\Phi}_1(\omega - \omega_s)}. \tag{2}$$

Since both LCFBG1 and LCFBG2 are fabricated with low reflectivities, the reflection spectrum of the FP interferometer should have an interference pattern within the reflection spectrum of LCFBG1 and LCFBG2. A simulated spectrum of an FP interferometer formed by two identical LCFBGs, with an identical reflectivity of 10% and a bandwidth of 4 nm centering at 1551 nm, is given in Fig. 2. For comparison, an ideal linearly chirped sinusoidal function is also shown (in log scale). It can be seen that such an FP interferometer has a spectral response that is similar to the shape of a sinusoidal function with an increasing period (or free spectral range) given by (2). The spectral response of the FP interferometer can thus be written as

$$\begin{aligned} R(\omega) &= \sin\left(\frac{2\pi}{\omega_{\text{FSR}}}\omega + \varphi\right) \\ &= \sin\left[\left(\frac{2n_{\text{eff}} d}{c} - 4\ddot{\Phi}_1\omega_s\right)\omega + 4\ddot{\Phi}_1\omega^2 + \varphi\right] \end{aligned} \tag{3}$$

where φ is an initial phase that will be interpreted as a microwave phase in the generated waveform. It can be seen from (2) and (3) that the free spectral range of the FP interferometer is linearly increasing or decreasing, depending on the sign of $\ddot{\Phi}_1$.

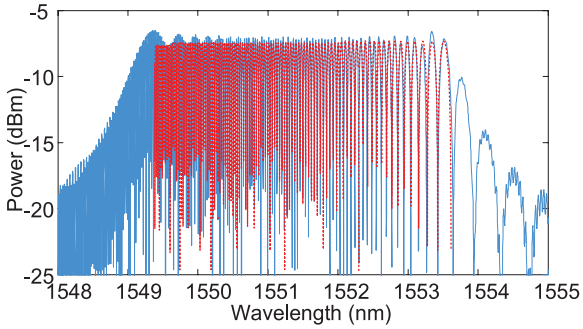

Fig. 2. Simulated reflection spectrum of an FP interferometer formed by two LCFBGs with complementary dispersion (solid line). The central wavelength and bandwidth of the two LCFBGs are 1551 and 4 nm. They are fabricated to have a uniform reflectivity of 10% and physically separated by 2 mm. The dotted line is an ideal linearly chirped microwave waveform.

After spectral shaping by the FP interferometer and amplification by EDFA1, the spectrally shaped pulse is directed into the dispersive loop via the optical coupler. It has been theoretically proven in [27] that the dispersive loop has an equivalent dispersion coefficient of $N\ddot{\Phi}_3$ thanks to the multi-time use of LCFBG3, where $\ddot{\Phi}_3$ and N are the dispersion coefficient of LCFBG3 and the round-trip number that the optical pulse travels in the loop, respectively. If the gain of EDFA2 can be controlled to fully compensate for the round-trip loss of the dispersive loop, N can be an extremely large number, which would result in a very large equivalent dispersion coefficient, hence, allowing a highly extended temporal duration for the generated linearly chirped microwave waveform.

When the pulse recirculates in the loop, wavelength-to-time mapping is performed. After N round trips, the electrical field at the output of the dispersive loop is given by [8]

$$y(t) = \exp\left(j\frac{1}{2N\ddot{\Phi}_3}t^2\right) X(\omega)\Big|_{\omega = t/N\ddot{\Phi}_3} \tag{4}$$

where $X(\omega) = G(\omega) \cdot R(\omega)$ is the optical spectrum of the pulse after being spectrally shaped by the FP interferometer, and $G(\omega)$ is the spectrum of a pulse from the MLL. In our case, the bandwidth of the pulse from the MLL is significantly larger than that of the optical spectral shaper, we can let $G(\omega) = 1$ for simplicity. In addition, the phase term in (4) will be eliminated by photo-detecting at a photodetector. Substituting (3) into (4), we get

$$y(t) = \sin\left(\frac{2n_{\text{eff}} d - 4c\ddot{\Phi}_1\omega_s}{cN\ddot{\Phi}_3}t + \frac{4\ddot{\Phi}_1}{N^2\ddot{\Phi}_3^2}t^2 + \varphi\right) \tag{5}$$

which precisely represents a linearly chirped microwave waveform with an instantaneous frequency of

$$f(t) = \frac{n_{\text{eff}} d - 2c\ddot{\Phi}_1\omega_s}{\pi cN\ddot{\Phi}_3} + \frac{4\ddot{\Phi}_1}{\pi N^2\ddot{\Phi}_3^2}t. \tag{6}$$

The first term of (6) determines the central frequency of the linearly chirped microwave waveform, while the second term corresponds to the linear frequency chirping. The central frequency of the linearly chirped microwave waveform can

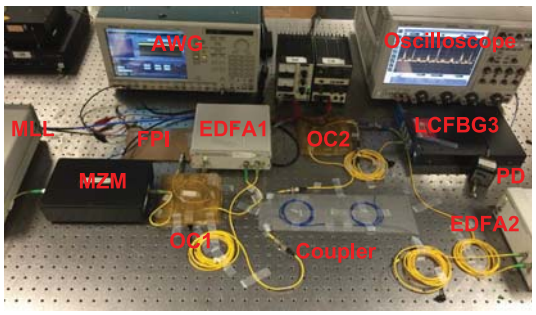

Fig. 3. Photograph of the experimental setup.

be changed by adjusting the spacing between LCFBG1 and LCFBG2.

In our system, the optical bandwidth is limited by the FP interferometer. Thus, it is required in (4) that

$$\omega_s \leq \frac{t}{N\ddot{\Phi}_3} \leq \omega_l \tag{7}$$

where ω_l denotes the upper frequency limit of the reflection bands of LCFBG1 and LCFBG2. The temporal duration of the linearly chirped microwave waveform can then be deduced from (7),

$$\Delta\tau = N\ddot{\Phi}_3 \Delta\omega \tag{8}$$

where $\Delta\omega = \omega_l - \omega_s$ is the bandwidth of the FP interferometer. Substituting (7) into (6), the bandwidth of the generated waveform is derived, which is given by

$$\Delta f = \frac{4\ddot{\Phi}_1 \Delta\omega}{\pi N\ddot{\Phi}_3}. \tag{9}$$

Multiplying (8) and (9), we get the TBWP,

$$\text{TBWP} = \frac{4\ddot{\Phi}_1 \Delta\omega^2}{\pi}. \tag{10}$$

It is seen that the TBWP of the linearly chirped microwave waveform is a constant even when the temporal duration is extended since the bandwidth of the waveform is reduced when the waveform is temporally extended. The product between the two remains constant. This conclusion is true for linear temporal stretching. However, the use of the dispersive loop allows us to generate a linearly chirped microwave waveform with a time duration that is N times as long as the one without a dispersive loop, and the TBWP can be controlled to be large by designing an FP interferometer with a wider bandwidth.

The central frequency of the generated linearly chirped microwave waveform can be tuned by adjusting the physical spacing between LCFBG1 and LCFBG2. A greater spacing corresponds to a higher central frequency. On the other hand, the bandwidth of the linearly chirped microwave waveform can be increased if the two LCFBGs in the FP interferometer are designed to have larger dispersion coefficients, which leads to an FP interferometer with a faster varying free spectral range.

III. Experiment

The linearly chirped microwave waveform generation system shown in Fig. 1 is then implemented. Fig. 3 gives a photograph of the experimental setup. An ultra-short optical pulse train is generated by an MLL (PriTel FFL-1550-20). The repetition rate and the central wavelength of the pulse train are 20 MHz and 1551.5 nm, respectively. The 3-dB spectral bandwidth of an individual pulse is 6 nm with a transform limited temporal width of 550 fs. The gate signal with a repetition rate of 1.18 MHz or a repetition period of 850 ns produced by the AWG (Tektronix AWG7102) provides a 50-ns-long time window to reduce the repetition rate of the pulse train from 20 to 1.18 MHz. The MZM is configured to operate as an optical switch, by biasing it at its minimum transmission point (switch off) and the maximum transmission point (switch on), corresponding to the gate is close and open, respectively. Note that if the MLL has a smaller repetition rate, the AWG and the MZM will not be needed and the system can be simplified. LCFBG1 and LCFBG2 forming the FP interferometer are fabricated to have a bandwidth of 4 nm centered at 1551.5 nm and a dispersion coefficient of ± 25 ps^2/rad. Two grating pairs with two different physical separations of 2 mm and 2 cm between LCFBG1 and LCFBG2 are fabricated to generate linearly chirped microwave waveforms with two different central frequencies. The reflection spectra of the two FP interferometers are shown in Fig. 4(a) and (b). A linearly increasing free spectral range is observed for both FP interferometers. The FP interferometer with a larger physical separation, i.e., longer FP interferometer cavity, has a smaller free spectral range that can be used for the generation of a linearly chirped microwave waveform with a higher central frequency. In the reflection spectra shown in Fig. 4(a) and (b), strong amplitude ripples are observed, especially for the smaller the free spectral range end.

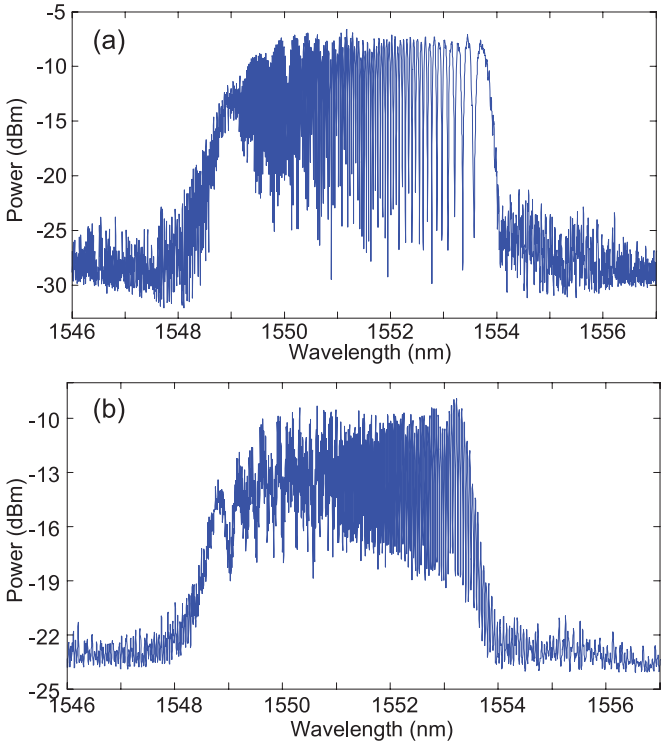

Fig. 4. Reflection spectra of the FP interferometers with a physical spacing between LCFBG1 and LCFBG2 of: (a) 2 mm and (b) 2 cm.

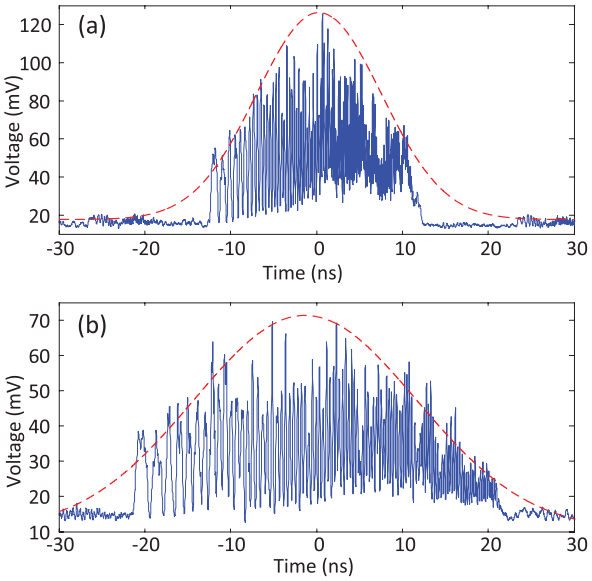

Fig. 5. Generated linearly chirped microwave waveforms using the FP interferometer with a physical spacing between the two LCFBGS of 2 mm with: (a) three and (b) five round trips.

The ripples are introduced by the limited wavelength sampling interval of the optical vector analyzer (LUNA Technologies) used to measure the spectra of the FP interferometers. The wavelength sampling interval is 2.4 pm, while the smallest free spectral range is 13 pm. LCFBG3 in the dispersive loop is fabricated to have a 4-nm reflection bandwidth with a center wavelength of 1551.5 nm and an in-band dispersion coefficient of -3188 ps^2/rad. Thanks to the multi-time use of LCFBG3 in the loop, a large equivalent dispersion coefficient can be achieved. For example, if the pulse is recirculating in the loop for five round trips, the equivalent dispersion coefficient would be as large as 15940 ps/nm. A photodetector (New Focus 1414, 20-GHz bandwidth) is used to detect the temporally stretched optical pulse to get a microwave waveform.

It should be noted that two EDFAs are used in the system. The first EDFA is required by the repetition-rate-reduction module to compensate for the insertion loss in the module. Since only 1 out of 17 pulses is selected by the MZM, the reduction in the repetition rate would introduce 12.3-dB insertion loss. If the insertion loss of the MZM of 5 dB is included, the total insertion loss is 17.3 dB. If the pulse train generated by the MLL has a longer repetition period, the first EDFA and the MZM will not be needed, and the system will be simplified. The insertion loss of the FP interferometer is 7.5 dB. The second EDFA is also required to compensate for the round-trip loss, to allow the pulse to recirculate for more round trips in the dispersive loop.

The linearly chirped microwave waveform generated at the photodetector is monitored by an oscilloscope (Agilent DSO-X 93204A). First, we use the FP interferometer with a separation of $d = 2$ mm as the optical spectral shaper. Fig. 5 shows two linearly chirped microwave waveforms after the pulse recirculates for three and five round trips in the loop. The linearly chirped microwave waveforms have decreasing periods, indicating a frequency up-chirp. Compared with

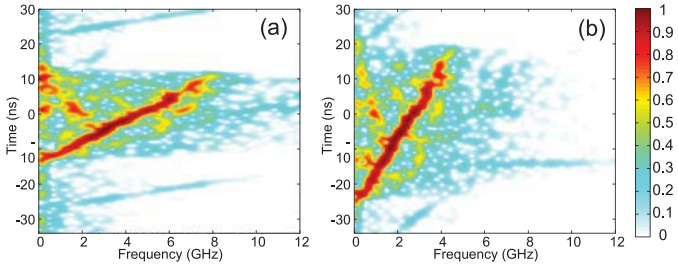

Fig. 6. Spectrograms of the linearly chirped microwave waveforms for: (a) three and (b) five round trips. The color scale represents the normalized amplitude of the spectrogram.

a single-time use of LCFBG3 that would generate a linearly chirped microwave waveform with a duration of less than 10 ns, extended temporal durations of around 25 and 42 ns are obtained for the two linearly chirped microwave waveforms. It should be noted that the waveforms should have temporal durations of 30 and 50 ns calculated theoretically based on (8). The differences in the temporal durations are due to the errors in the fabrication of the LCFBGs, which would cause a reflection band mismatch between the LCFBGs. The amplitude ripples shown in the linearly chirped microwave waveform spectra are resulted from the ripples in the spectrum of an MLL pulse, the non-flat gain spectra of the EDFAs, and the ripples in the reflection spectra of the LCFBGs. There ripples can be mitigated by adding an optical gain-flattening filter in the dispersive loop.

The spectrograms of the generated linearly chirped microwave waveforms shown in Fig. 5 are calculated and shown in Fig. 6. Linearly increasing instantaneous frequencies can be observed for the two generated linearly chirped microwave waveforms, which indicate a good linearity of the frequency chirping of the waveforms. The two linearly chirped microwave waveforms have bandwidths of 8.4 and 5.0 GHz with an identical TBWP of around 210. However, the temporal durations are extended thanks to the greater equivalent dispersion coefficient of the dispersive loop. According to (10), the theoretical TBWP of the system is estimated to be 315. Since wavelength-to-time mapping is only performed to part of the spectrum (82%, in our case) shown in Fig. 4 due to the mismatch between the reflection bandwidths of the LCFBGs, the temporal durations and bandwidths of the linearly chirped microwave waveforms are reduced.

In a radar receiver, a linearly chirped microwave waveform is compressed by a matched filter to improve the range resolution. The calculated correlation results between a linearly chirped microwave waveform and its reference are presented in Fig. 7(a) and (b). The widths of the correlation peaks are 100 and 160 ps for the two linearly chirped microwave waveforms after three and five round trips, which correspond to two suppression ratios of 250 and 262, respectively.

To generate a linearly chirped microwave waveform at a different frequency band, a second FP interferometer with a physical separation of $d = 2$ cm is then employed as the optical spectral shaper. The linearly chirped microwave waveform for five round trips are shown in Fig. 8(a). A 45-ns-long linearly chirped microwave waveform is achieved. The minimum

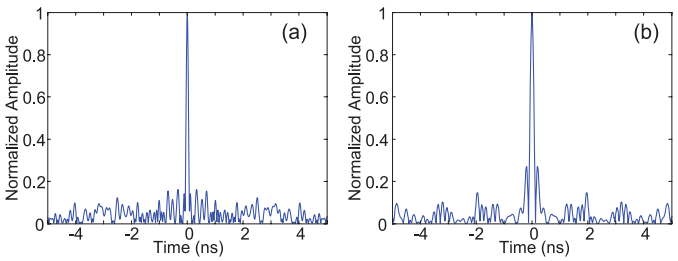

Fig. 7. Calculated autocorrelation between the linearly chirped microwave waveforms and their references. For the FP interferometer with a spacing of: (a) 2 mm and (b) 2 cm.

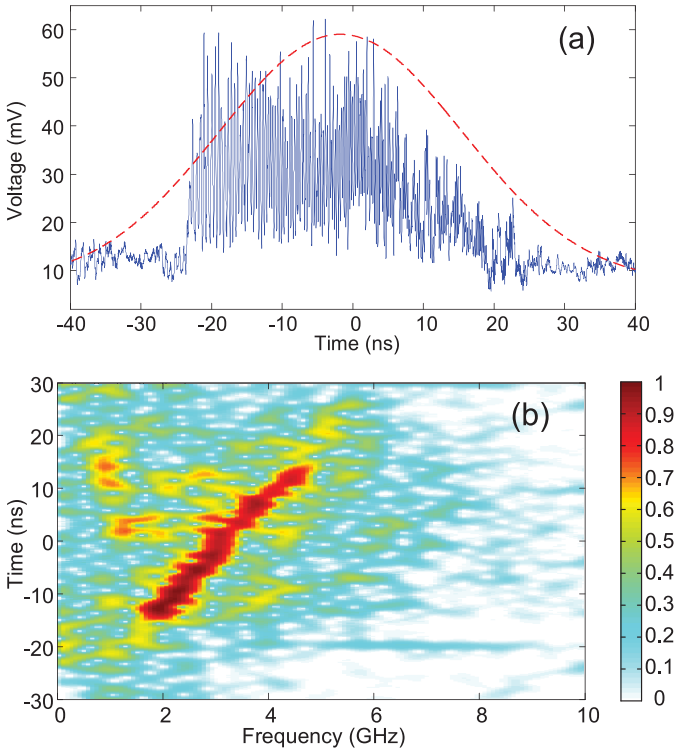

Fig. 8. (a) Generated linearly chirped microwave waveform using the FP interferometer with a spacing of 2 cm after the optical pulse recirculates for five round trips and (b) corresponding spectrogram. The color scale represents the normalized amplitude of the spectrogram.

frequency is 1.5 GHz instead of around dc for the linearly chirped microwave waveform shown in Fig. 5. However, strong attenuation can be observed for the high-frequency components due to a lower responsivity of the photodetector at a higher frequency band. The spectrogram in Fig. 8(b) indicates a TBWP of only 180, which is also caused by the lower responsivity of the photodetector at the higher frequency band. The calculated autocorrelation of the linearly chirped microwave waveform shows a width of the correlation peak of 358 ps. A compression ratio of 125 is achieved for the 45-ns long linearly chirped microwave waveforms. It should be noted that amplitude ripples in the spectra of the linearly chirped microwave waveforms shown in Figs. 5 and 8 are observed. The ripples are caused due to the lasing in the dispersive loop since the gains at certain wavelengths are near the lasing threshold. To reduce the ripples, in the dispersive loop, a gain-flattening filter may be used to flatten the gain spectrum of the EDFA so that the lasing can be suppressed.

The stability of the proposed linearly chirped microwave waveform generator is also studied. We first investigate the short-term stability. To do so, two linearly chirped microwave waveforms that are separated in time by 60 cycles (45 μs) are sampled and compared. The linearly chirped microwave waveforms have very similar shapes, including the amplitude ripples and the phase responses, indicating good stability and repeatability of the operation of the system. The cross-correlation between the two linearly chirped microwave waveforms is also calculated, which is identical to the autocorrelation of one of the linearly chirped microwave waveforms. This again demonstrates a stable and repeatable operation of the system. The long-term stability is strongly affected by the ambient temperature change, as the FP interferometer is temperature sensitive. By using a temperature control unit, the long-term stability can be improved.

IV. Conclusion

An approach to the generation of a linearly chirped microwave waveform with an extended temporal duration implemented by an FP interferometer for spectral shaping and a dispersive loop for wavelength-to-time mapping was proposed and experimentally demonstrated. Long temporal duration for the generated linearly chirped microwave waveform was enabled by multi-time use of an LCFBG in a dispersive to perform wavelength-to-time mapping. Two linearly chirped microwave waveforms with two temporal widths of 25 and 42 ns were generated at two different frequency bands. A further increase in the temporal durations of the linearly chirped microwave waveforms is possible by allowing the optical pulse recirculate for more round trips in the loop. The TBWPs of the two linearly chirped microwave waveforms were both 210 and the extension of the temporal duration of a linearly chirped microwave waveform will not increase the TBWP for a given FP interferometer. To increase the TBWP, an FP interferometer with two LCFBGs having larger dispersion coefficients may be used. For example, if two LCFBGs with two opposite dispersion coefficients of ± 3188 ps^2 are used to constitute the FP interferometer and a photodetector with a bandwidth of over 100 GHz is used to perform photodetection [18], a linearly chirped microwave waveform with a TBWP as large as 4200 can be generated.

References

[1] D. K. Barton, *Radar System Analysis and Modeling*. Norwood, MA, USA: Artech House, 2004.
[2] A. W. Rihaczek, *Principles of High-Resolution Radar*. New York, NY, USA: McGraw-Hill, 1969.
[3] R. Skaug and J. F. Hjelmstad, *Spread Spectrum in Communication*. London, U.K.: IET, 1985.
[4] M. Bertero, M. Miyakawa, P. Boccacci, F. Conte, K. Orikasa, and M. Furutani, "Image restoration in chirp-pulse microwave CT (CP-MCT)," *IEEE Trans. Biomed. Eng.*, vol. 47, no. 5, pp. 690–699, May 2000.
[5] J. Levy, P. Burke, L. Cohen, and R. Cecchini, "VCO based chirp generation for broad bandwidth compressive receiver applications (in EW)," in *IEEE MTT-S Int. Microw. Symp. Dig.*, Jun. 1993, vol. 3, pp. 1113–1115.

[6] A. Stelzer, K. Ettinger, J. Hoftberger, J. Fenk, and R. Weigel, "Fast and accurate ramp generation with a PLL-stabilized 24-GHz SiGe VCO for FMCW and FSCW applications," in *IEEE MTT-S Int. Microw. Symp. Dig.*, Jun. 2003, vol. 2, pp. 893–896.

[7] D. Gomez-Garcia, C. Leuschen, F. Rodriguez-Morales, J.-B. Yan, and P. Gogineni, "Linear chirp generator based on direct digital synthesis and frequency multiplication for airborne FMCW snow probing radar," in *IEEE MTT-S Int. Microw. Symp. Dig.*, Jun. 2014, pp. 1–4.

[8] J. Yao, "Photonic generation of microwave arbitrary waveforms," *Opt. Commun.*, vol. 284, no. 15, pp. 3723–3736, Jul. 2011.

[9] J. D. McKinney, D. Seo, D. E. Leaird, and A. M. Weiner, "Photonically assisted generation of arbitrary millimeter-wave and microwave electromagnetic waveforms via direct space-to-time optical pulse shaping," *J. Lightw. Technol.*, vol. 21, no. 12, pp. 3020–3028, Dec. 2003.

[10] S. T. Cundiff and A. M. Weiner, "Optical arbitrary waveform generation," *Nature Photon.*, vol. 4, pp. 760–766, Oct. 2010.

[11] A. Vega, D. E. Leaird, and A. M. Weiner, "High-speed direct space-to-time pulse shaping with 1 ns reconfiguration," *Opt. Lett.*, vol. 35, no. 10, pp. 1554–1556, May 2010.

[12] A. Zeitouny, S. Stepanov, O. Levinson, and M. Horowitz, "Optical generation of linearly chirped microwave pulses using fiber Bragg gratings," *IEEE Photon. Technol. Lett.*, vol. 17, no. 3, pp. 660–662, Mar. 2005.

[13] C. Wang and J. P. Yao, "Photonic generation of chirped microwave pulses using superimposed chirped fiber Bragg gratings," *IEEE Photon. Technol. Lett.*, vol. 20, no. 11, pp. 882–884, Jun. 2008.

[14] C. Wang and J. P. Yao, "Chirped microwave pulse generation based on optical spectral shaping and wavelength-to-time mapping using a Sagnac-loop mirror incorporating a chirped fiber Bragg grating," *J. Lightw. Technol.*, vol. 27, no. 16, pp. 3336–3341, Aug. 2009.

[15] H. Shahoei and J. P. Yao, "Continuously tunable chirped microwave waveform generation using a tilted fiber Bragg grating written in an erbium/ytterbium co-doped fiber," *IEEE Photon. J.*, vol. 4, no. 3, pp. 765–771, Jun. 2012.

[16] M. H. Khan *et al.*, "Ultrabroad-bandwidth arbitrary radiofrequency waveform generation with a silicon photonic chip-based spectral shaper," *Nature Photon.*, vol. 4, no. 2, pp. 117–122, Feb. 2010.

[17] A. Rashidinejad and A. M. Weiner, "Photonic radio-frequency arbitrary waveform generation with maximal time-bandwidth product capability," *J. Lightw. Technol.*, vol. 32, no. 20, pp. 3383–3393, Oct. 2014.

[18] Y. Li, A. Rashidinejad, J.-M. Wun, D. E. Leaird, J.-W. Shi, and A. M. Weiner, "Photonic generation of W-band arbitrary waveforms with high time-bandwidth products enabling 3.9 mm range resolution," *Optica*, vol. 1, no. 6, pp. 446–454, Dec. 2014.

[19] Y. Li, A. Dezfooliyan, and A. M. Weiner, "Photonic synthesis of spread spectrum radio frequency waveforms with arbitrarily long time apertures," *J. Lightw. Technol.*, vol. 32, no. 20, pp. 3580–3587, Oct. 2014.

[20] J. Azaña, N. K. Berger, B. Levit, and B. Fischer, "Reconfigurable generation of high-repetition-rate optical pulse sequences based on time-domain phase-only filtering," *Opt. Lett.*, vol. 30, no. 23, pp. 3228–3230, Dec. 2005.

[21] O. L. Coutinho, J. Zhang, and J. Yao, "Photonic generation of a linearly chirped microwave waveform with a large time-bandwidth product based on self-heterodyne technique," in *IEEE Int. Microw. Photon. Top. Meeting*, Oct. 2105, pp. 1–4.

[22] Y. Dai and J. Yao, "Chirped microwave pulse generation using a photonic microwave delay-line filter with a quadratic phase response," *IEEE Photon. Technol. Lett.*, vol. 21, no. 9, pp. 569–571, May 2009.

[23] W. Li and J. P. Yao, "Generation of linearly chirped microwave waveform with an increased time-bandwidth product based on a tunable optoelectronic oscillator and a recirculating phase modulation loop," *J. Lightw. Technol.*, vol. 32, no. 20, pp. 3573–3579, Oct. 2014.

[24] T. Erdogan, "Fiber grating spectra," *J. Lightw. Technol.*, vol. 15, no. 8, pp. 1277–1294, Aug. 1997.

[25] J. Chou, O. Boyraz, D. Solli, and B. Jalali, "Femtosecond real-time single-shot digitizer," *Appl. Phys. Lett.*, vol. 91, no. 16, pp. 161105–161105, Oct. 2007.

[26] J. Zhang, O. L. Coutinho, and J. Yao, "Photonic generation of a linearly chirped microwave waveform with long temporal duration using a dispersive loop," in *IEEE MTT-S Int. Microw. Symp. Dig.*, May 2015, pp. 1–3, TU3G-2.

[27] J. Zhang and J. P. Yao, "Time stretched sampling of a fast microwave waveform based on the repetitive use of a linearly chirped fiber Bragg grating in a dispersive loop," *Optica*, vol. 1, no. 2, pp. 64–69, Aug. 2014.

Jiejun Zhang (S'12) received the B.Eng. degree in electronic science and technology from the Harbin Institute of Technology, Harbin, China, in 2010, the M.Sc. degree in optical engineering from the Huazhong University of Science and Technology, Wuhan, China, in 2010, and is currently working toward the Ph.D. degree at the University of Ottawa, Ottawa, ON, Canada.

He is currently with the Microwave Photonics Research Laboratory, School of Electrical Engineering and Computer Science, University of Ottawa. His research interests include photonic generation of microwave waveforms, photonic processing of microwave signals, and fiber-optic sensors.

Olympio Lucchini Coutinho (M'15) received the B.Eng. degree in electrical engineering from the Pontifícia Universidade Católica de Minas Gerais, Belo Horizonte, Brazil, in 1993, and the M.Sc. and Ph.D. degrees in electronic and computing engineering from the Technological Institute of Aeronautics, São José dos Campos, Brazil, in 2005 and 2011, respectively.

He is currently a Postdoctoral Fellow with the Microwave Photonic Research Laboratory, School of Electrical Engineering and Computer Science, University of Ottawa, Ottawa, ON, Canada, sponsored by the Technological Institute of Aeronautics, Brazil, where he is an Adjunct Professor and Researcher. His research interests include photonic generation, transmission and processing of microwave signals for radar applications, as well as fiber optic sensors.

Dr. Coutinho is a Member of the Brazilian Microwave and Optoelectronic Society.

Jianping Yao (M'99–SM'01–F'12) received the Ph.D. degree in electrical engineering from the Université de Toulon et du Var, La Garde, France, in 1997.

He is currently a Professor and University Research Chair with the School of Electrical Engineering and Computer Science, University of Ottawa, Ottawa, ON, Canada. From 1998 to 2001, he was with the School of Electrical and Electronic Engineering, Nanyang Technological University (NTU), Singapore, as an Assistant Professor. In December 2001, he joined the School of Electrical Engineering and Computer Science, University of Ottawa, as an Assistant Professor, where he became an Associate Professor in 2003, and a Full Professor in 2006. In 2007, he became University Research Chair in Microwave Photonics. From July 2007 to June 2010, he was the Director of the Ottawa–Carleton Institute for Electrical and Computer Engineering. In 2013, he was re-appointed Director of the Ottawa-Carleton Institute for Electrical and Computer Engineering. He has authored or coauthored more than 510 research papers, including more than 300 papers in peer-reviewed journals and 210 papers in conference proceedings.

Prof. Yao is a Registered Professional Engineer in the Province of Ontario. He is a Fellow of the Optical Society of America and the Canadian Academy of Engineering. He is a Topical Editor for *Optics Letters* and serves on the Editorial Board of the IEEE TRANSACTIONS ON MICROWAVE THEORY AND TECHNIQUES, *Optics Communications*, *Frontiers of Optoelectronics*, and *Science Bulletin*. He was a Guest Co-Editor for a Focus Issue on Microwave Photonics in *Optics Express* in 2013 and a Lead-Editor for a Feature Issue on Microwave Photonics in *Photonics Research* in 2014. He has been a Chair of numerous international conferences, symposia, and workshops, including the Vice Technical Program Committee (TPC) Chair of the IEEE Microwave Photonics Conference in 2007, TPC Co-Chair of the Asia–Pacific Microwave Photonics Conference in 2009 and 2010, TPC Chair of the High-Speed and Broadband Wireless Technologies Subcommittee of the IEEE Radio Wireless Symposium in 2009–2012, TPC Chair of the Microwave Photonics Subcommittee of the IEEE Photonics Society Annual Meeting in 2009, TPC Chair of the IEEE Microwave Photonics Conference in 2010, General Co-Chair of the IEEE Microwave Photonics Conference in 2011, TPC Co-Chair of the IEEE Microwave Photonics Conference in 2014, and General Co-Chair of the IEEE Microwave Photonics Conference in 2015. He has also been a Committee Member of numerous international conferences such as IPC, OFC, BGPP, and MWP. He was an IEEE Microwave Theory and Techniques Society (IEEE MTT-S) Distinguished Microwave Lecturer (2013–2015). He was the recipient of the 2005 International Creative Research Award of the University of Ottawa, the 2007 George S. Glinski Award for Excellence in Research, the 2008 Natural Sciences and Engineering Research Council of Canada Discovery Accelerator Supplements Award, and the inaugural 2012 OSA Outstanding Reviewer Award.